Human Reproduction, Vol.27, No.S1 pp. i2–i21, 2012
doi:10.1093/humrep/des200

human reproduction

CHAPTER ONE

The oocyte

Laura Rienzi, Basak Balaban, Thomas Ebner and Jacqueline Mandelbaum

Contents

Introduction

The female gamete plays a crucial role in determining embryo competence and therefore *in vitro* fertilization (IVF) results. Oocyte quality is not only influenced by the nuclear and mitochondrial genome, but also by the microenvironment provided by the ovary and the pre-ovulatory follicle that influences transcription and translation, and as a consequence, cytoplasmic maturity. In contrast to *in vivo* processes, the application of ovarian hormone stimulation protocols for IVF bypasses the complicated selection procedure that usually occurs during oocyte development and maturation of a single oocyte for ovulation, and allows for the maturation of many oocytes, often with compromised quality.

It has been speculated (Van Blerkom and Henry, 1992) that some morphological irregularities, which can easily be assessed at the light microscopy level, may reflect a compromised developmental ability of the oocytes and could therefore represent a useful tool for selecting competent oocytes prior to fertilization. Oocyte morphological assessment in the laboratory is first based on the presentation of the cumulus–corona cells. For mature oocytes, the cumulus–corona mass should appear as an expanded and mucified layer, due to active secretion of hyaluronic acid. This extracellular matrix molecule interposes between the cumulus cells (CCs), separating them and conferring to the cumulus–corona mass a fluffy 'cloud-like' appearance. However, stimulated cycles may be characterized by asynchrony between the nuclear maturation status of the oocyte and the expansion of the cumulus–corona cell mass. This has been suggested to be caused by a different sensitivity of the oocyte and the cumulus–corona mass to the stimulants (Laufer *et al.*, 1984).

Following the removal of the cumulus–corona cells in preparation for intracytoplasmic sperm injection (ICSI), oocyte evaluation is more accurate and is based on the nuclear maturation status, the morphology of the cytoplasm and on the appearance of the extracytoplasmic structures. The presence of the first polar body (PBI) is normally considered to be a marker of oocyte nuclear maturity. However, recent studies using polarized light microscopy have shown that oocytes displaying a polar body may still be immature (Rienzi *et al.*, 2005). Only those displaying a meiotic spindle (MS) can in fact be considered as true, mature, Metaphase II (MII) stage oocytes. The presence, position and retardance of the MS have been suggested to be related to developmental competence. In accordance with a recent meta-analysis (Petersen *et al.*, 2009), however, only *in vitro* development can be related to the morphology of the MS. Analyses of *in vivo* development are relatively rare in the literature and the meta-analysis failed to show significant differences in implantation rates between embryos derived from oocytes displaying a detectable MS and those without.

Nuclear maturity alone is, in fact, not enough to determine the quality of an oocyte. Nuclear and cytoplasmic maturation should be completed in a coordinated manner to ensure optimal conditions for subsequent fertilization. An ideal mature human oocyte, based on morphological characteristics, should have a 'normal-looking' cytoplasm, a single polar body, an appropriate zona pellucida (ZP) thickness and proper perivitelline space (PVS; Swain and Pool, 2008). However, the majority of the oocytes retrieved after ovarian hyperstimulation exhibit one or more variations in the described 'ideal' morphological criteria (De Sutter *et al.*, 1996; Xia, 1997; Balaban *et al.*, 1998; Mikkelsen and Lindenberg, 2001; Balaban and Urman, 2006; Ebner *et al.*, 2006; Rienzi *et al.*, 2008). This is also true for oocytes obtained from proven fertile donors (Ten *et al.*, 2007). Morphology, moreover, often fails to predict fertilizing ability and developmental competence (Rienzi *et al.*, 2011). Only a few morphologically detectable features of the Metaphase II oocyte indicate compromised developmental ability. According to the Istanbul consensus workshop on embryo assessment (Alpha Scientists in Reproductive Medicine and ESHRE Special Interest Group of Embryology, 2011) extracytoplasmic anomalies (PBI morphology, PVS size, the appearance of the ZP) are simply phenotypic variations often related to *in vitro* culture and/or oocyte aging. On the other hand, a special deviation in the cytoplasmic texture, namely the presence of aggregations of smooth endoplasmic reticulum (SER) is potentially lethal and developmental competence of

these oocytes should be interpreted with caution. Oocyte morphology may also reflect genetic abnormalities. This is the case for giant oocytes that contain one additional set of chromosomes. These oocytes, when observed with polarized light microscopy, display two distinct MS. Although, the occurrence of giant oocytes is relatively rare after ovarian hyperstimulation, the use of these cells for IVF is dangerous.

Owing to the complex mechanisms related to oocyte maturation and acquisition of competence, it is unlikely that a single characteristic (with the exception of oocyte size and the presence of SER aggregates) can adequately reflect the quality of the cell. Accordingly, to obtain information about the competence of the oocyte, morphological assessment should be combined with other approaches (i.e. cumulus–corona cell gene expression, metabolomics and oxygen consumption). Further predictive value could be obtained by combining the oocyte evaluation with evaluations of preimplantation development (pronuclear stage, cleavage stage and blastocyst stage).

A. Cumulus-enclosed oocytes

During follicular antrum formation, granulosa cells (GCs) differentiate into mural GCs, lining the follicular wall, and CCs, surrounding the oocyte. Within the cumulus mass, CCs in close contact with the oocyte (corona cells) develop cytoplasmic projections which cross the ZP and form gap junctions with the oolemma. This organized structure is called the cumulus–oocyte complex (COC; Fig. 1; Albertini *et al.*, 2001). In natural spontaneous cycles, oocyte nuclear maturation runs parallel to the gradual FSH-dependent expansion of the cumulus and corona cells, whereas this synchrony may be disturbed in stimulated cycles (Laufer *et al.*, 1984). Immature COCs (Fig. 2), commonly retrieved from small follicles during *in vitro* maturation (IVM) cycles, show a typically unexpanded cumulus with multilayers of compact GCs adhering to the ZP of an immature oocyte at prophase I [germinal-vesicle stage (GV); Figs 3 and 4]. IVM of such immature COCs aims for expansion of CCs and oocyte nuclear maturation.

Figure 1 Cumulus–oocyte complex obtained following ovarian stimulation. The oocyte is typically surrounded by an expanded cumulus corona cell complex. Note the outer CCs separated from each other by extracellular matrix and the corona cells immediately adjacent to the oocyte becoming less compact and radiating away from the ZP. PB1 is located at the 1 o'clock position.

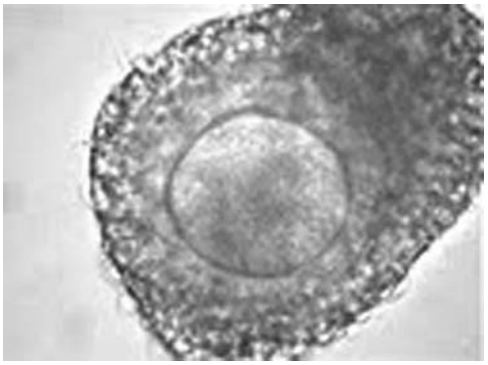

Figure 2 A cumulus–oocyte complex recovered from an IVM cycle showing an oocyte surrounded by unexpanded, compact cumulus and corona cells.

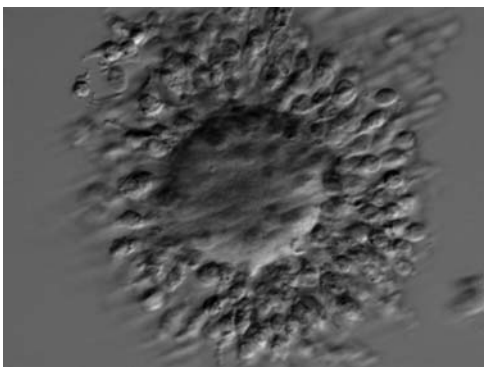

Figure 3 A cumulus–oocyte complex recovered from an IVM cycle. The immature GV oocyte is surrounded by compact GCs. The nucleolus in the GV is visible at the 10 o'clock position.

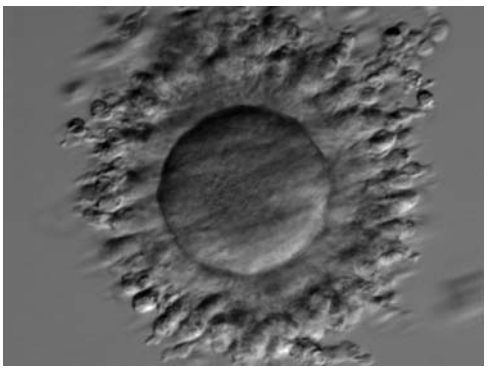

Figure 4 A cumulus–oocyte complex recovered from an IVM cycle. The immature oocyte has a GV at the 3 o'clock position with the nucleolus towards the centre of the oocyte. Compact GCs surround the oocyte.

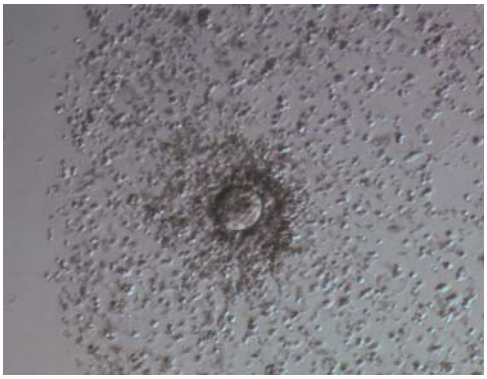

Figure 5 A cumulus oocyte complex at low magnification. The oocyte is surrounded by an expanded cumulus–corona cell complex clearly showing the separation of individual CCs due to the accumulation of hyaluronic acid in the extracellular space.

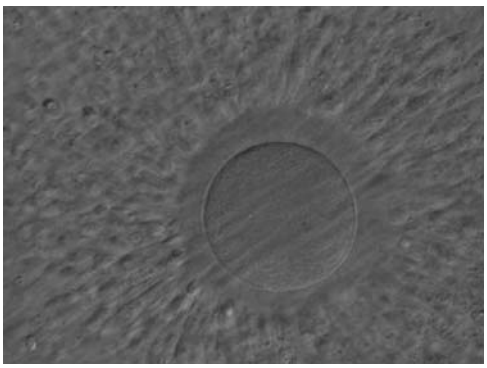

Figure 6 A cumulus–oocyte complex obtained following ovarian stimulation. An expanded cumulus corona cell complex surrounds the oocyte with the outer CCs separated from each other by extracellular matrix. The CCs immediately adjacent to the oocyte become less compact and radiate away from the ZP. The oocyte in the figure can be clearly seen through the surrounding cells at high magnification and no polar body can be seen in the PVS despite the mature status of the cumulus–corona cells.

In stimulated cycles, 34–38 h after triggering ovulation, a typical mature pre-ovulatory COC displays radiating corona cells surrounded by the expanded, loose mass of CCs (Fig. 5). In the majority of expanded COCs, oocytes are mature at the MII stage, although it is possible after gonadotrophin stimulation to find in a mucified cumulus and radiating corona cells an immature oocyte at the GV or metaphase I (MI) stage (Fig. 6). It is common, in stimulated cycles, to recover COCs with an expanded cumulus cell mass but compact, non-radiating corona cells (Figs 7a, 8a and 9a). Indeed, at recovery, the presence of the surrounding cumulus and corona cells usually prevents identification of the PBI in the PVS, an indicator of successful completion of meiosis I with arrest at the MII stage of development (Fig. 1). In preparation for ICSI, oocyte denudation is performed via enzymatic action of hyaluronidase (Figs 7b , 8b and 9b) and mechanical pipetting, allowing the accurate determination of the oocyte nuclear status (Figs 7c , 8c and 9c).

The Alpha-ESHRE consensus document states that, although there is little corroborated evidence to support a correlation between the appearance of the COC and embryo developmental competence, a binary score (0 or 1) with a 'good' COC (score 1) defined as having an expanded cumulus and a radiating corona should be documented (Alpha Scientists in Reproductive Medicine and ESHRE Special Interest Group of Embryology, 2011).

The bidirectional communication between the oocyte and CCs, crucial for the acquisition of oocyte competence (Gilchrist *et al.*, 2008), might perhaps be investigated in the future, through non-invasive analysis of CCs (pattern of gene expression or protein synthesis), offering new biomarkers of oocyte quality, compensating for the inadequacy of the COC morphological assessment (Feuerstein *et al.*, 2007; Ouandaogo *et al.*, 2011).

B. Oocyte maturation stage

The removal of the cumulus–corona cell mass gives the unique opportunity to evaluate oocyte morphology prior to fertilization, and in particular, the nuclear maturation stage. Oocyte nuclear maturity, as assessed by light microscopy, is assumed to be at the MII stage when the PBI is visible in the PVS (Figs 10 and 11). The MII stage is characterized by the alignment of the homologous chromosomes on the spindle equatorial plate during metaphase of the second meiotic division. It is generally recognized that 85% of the retrieved oocytes following ovarian hyperstimulation display the PBI and are classified as MII, whereas 10% present an intracytoplasmic nucleus called the 'germinal vesicle' (GV; Figs 12–14), characteristic of prophase I of the first meiotic division. Approximately 5% of the oocytes have neither a visible GV nor PBI and these oocytes are generally classified as MI oocytes (Figs 15–17; Rienzi and Ubaldi, 2009). These oocytes may, however, be at the GV breakdown stage where the nuclear envelope has broken down but has not as yet progressed to true MI where the chromosomes are aligned on the metaphase plate in preparation for the completion of the first meiotic division.

Additional information on oocyte nuclear status can be obtained with the use of polarized light microscopy combined with software for image processing for the non-invasive visualization of the MS and other oocyte birefringent structures. The MS is a microtubular structure involved in chromosome segregation, and therefore is crucial in the sequence of events leading to the correct completion of meiosis and subsequent fertilization. Parallel-aligned MS microtubules are birefringent and able to shift the plane of polarized light inducing a retardance; these properties enable the system to generate contrast and image the MS structure (Oldenbourg, 1999; Fig. 18). The presence of the MS gives more accurate information about the nuclear stage of the oocyte. In particular, some oocytes can be immature (at the stage of early telophase I) when observed with polarized light microscopy, despite the presence of PBI in the PVS. At this stage, in fact, there is continuity between the ooplasm of the oocyte and the forming PBI and the MS is interposed between the two separating cells (Figs 19–22). This condition normally has a duration of 75–90 min. The MS has been found to disappear in late telophase I (Fig. 23), reforming only 40–60 min later (Montag *et al.*, 2011). However, it must be underlined that other factors, such as sub-optimal culture conditions, temperature

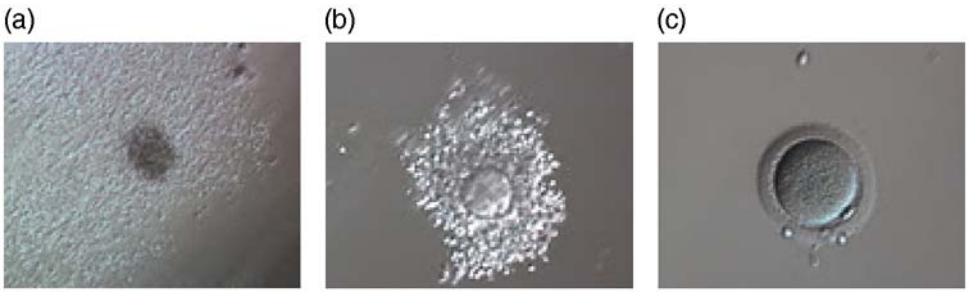

Figure 7 Denudation sequences of a mature oocyte. (**a**) Cumulus–corona oocyte complex before the denudation process with non-radiating CCs. (100× magnification). (**b**) Oocyte surrounded by corona cells during hyaluronidase treatment (200× magnification). (**c**) Denuded oocyte after mechanical stripping, a visible polar body is present in the PVS (200× magnification).

Figure 8 Denudation sequences of a mature oocyte. (**a**) Cumulus–corona oocyte complex before the denudation process (100× magnification). CCs are abundant. (**b**) Oocyte surrounded by corona cells during hyaluronidase treatment (200× magnification). Many CCs are still present, but the mature oocyte is already visible with PB1 at the 7 o'clock position. (**c**) Denuded oocyte after mechanical stripping, a visible polar body is present in the PVS (200× magnification).

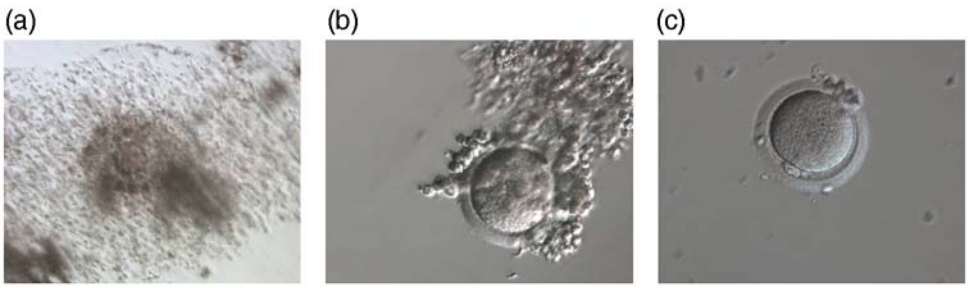

Figure 9 Denudation sequences of a mature oocyte. (**a**) Cumulus–corona oocyte complex before the denudation process with compact, non-radiating CCs. (100× magnification). (**b**) Oocyte surrounded by corona cells during hyaluronidase treatment (200× magnification). (**c**) Denuded oocyte after mechanical stripping, a visible polar body is present in the PVS (200× magnification).

fluctuations and chemical stress during manipulation, can contribute to MS disassembly (Rienzi and Ubaldi, 2009). Finally, the percentage of oocytes with detectable MS is also related to the time elapsed from HCG administration and is higher after 38 h (Cohen *et al.*, 2004). In general, it is expected that at least 80% of oocytes recovered following ovarian hyperstimulation are MS positive when viewed by polarized light microscopy.

C. Oocyte size and shape

A critical oocyte size is necessary for resumption of meiosis (Otoi *et al.*, 2000). At the beginning of oocyte growth, size is determined by strong adhesion between the oolemma and the inner zona surface (Tartia *et al.*, 2009). Around ovulation GLYT1 is activated

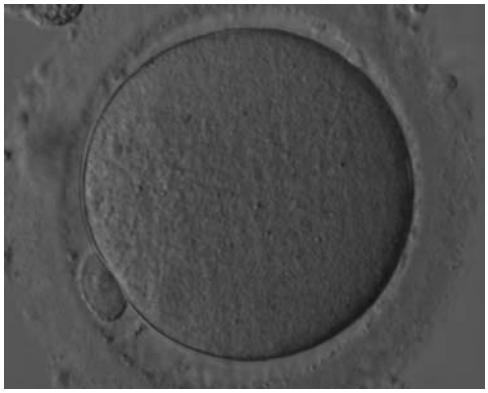

Figure 10 Denuded MII oocyte; an intact PBI is clearly visible in the PVS (400× magnification).

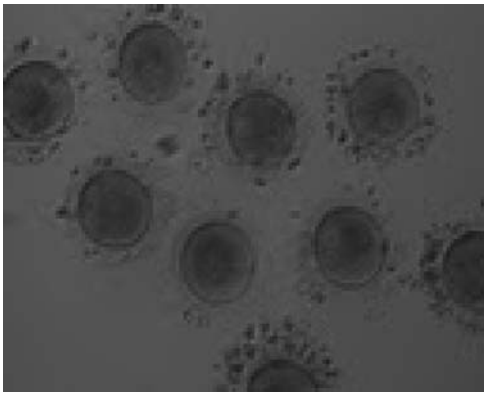

Figure 13 Denuded GV oocytes. Several GV with the organelles condensed centrally within the cytoplasm (200× magnification).

Figure 11 Denuded MII oocyte; the PBI is clearly visible in the narrow PVS (400× magnification).

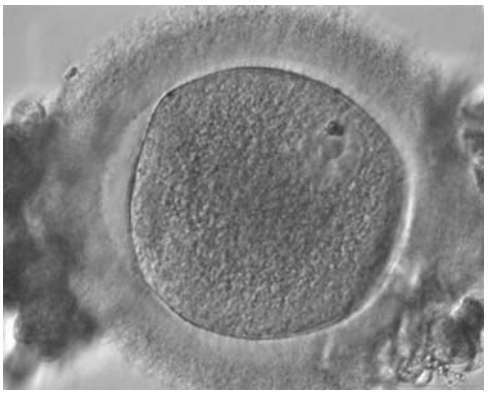

Figure 14 Denuded GV oocyte. A GV oocyte that is possibly approaching GVBD as the nuclear membrane is not distinct over its entirety (400× magnification).

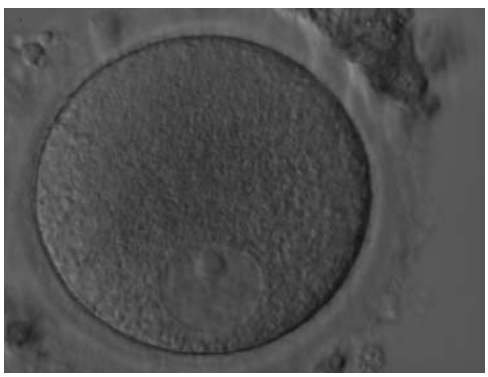

Figure 12 Denuded GV oocyte. A typical GV oocyte with an eccentrically placed nucleus and a prominent single nucleolus (400× magnification).

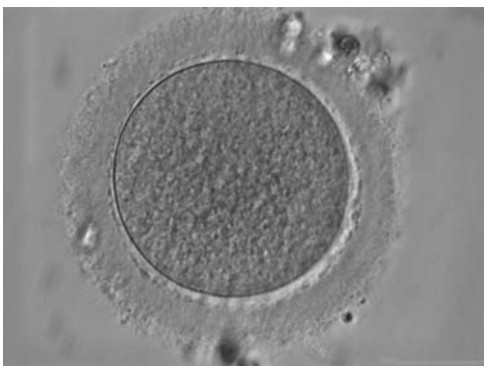

Figure 15 Denuded MI oocyte. This oocyte has no visible nucleus and has not as yet extruded the PBI (400× magnification). PVS is typically narrow.

Figure 16 Denuded MI oocyte with no visible nucleus and no PBI (400× magnification). Some CCs are still tightly adhered to the ZP.

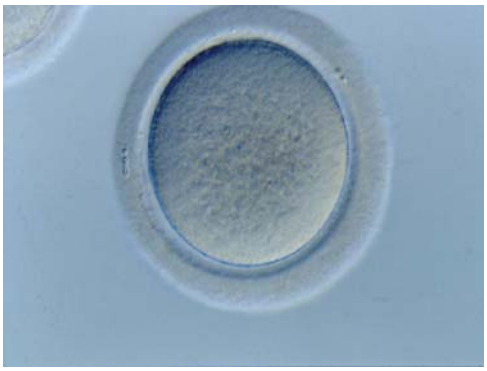

Figure 17 Denuded MI oocyte without a visible nucleus or an extruded PBI (400× magnification).

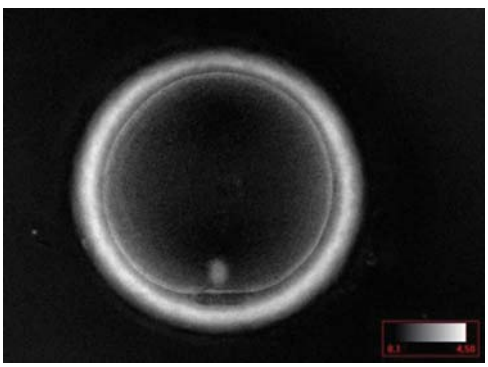

Figure 18 MII oocyte visualized using polarized light microscopy (400× magnification). The polar body is present at the 6 o'clock position in the PVS, and the MS of the second meiotic division is visible in the cytoplasm perfectly aligned to PB1 position. This is a fully mature MII oocyte.

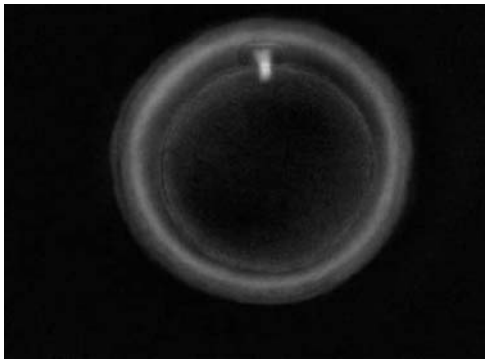

Figure 19 Telophase I oocyte visualized using polarized light microscopy (400× magnification). PB1 is present in the PVS; however, the MS can be seen between PB1 and the oocyte cytoplasm indicating that this oocyte is still completing the first meiotic division. This is not yet a fully mature MII oocyte.

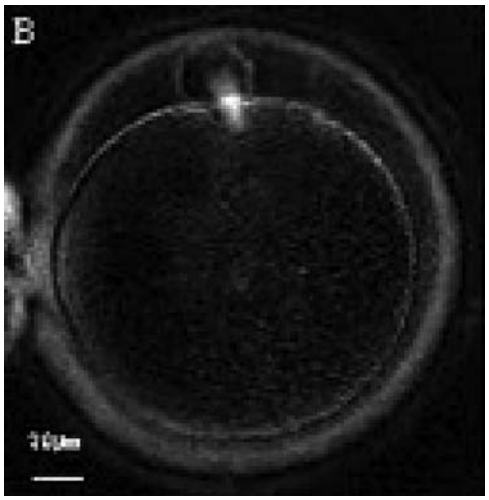

Figure 20 Telophase I oocyte visualized using polarized light microscopy (400× magnification). The MS can be seen between PB1 and the oocyte cytoplasm indicating that the first meiotic division is not yet completed.

which mediates glycin accumulation which in turn acts as an osmolyte and thus controls cell volume (Baltz and Tartia, 2009).

The mean ovarian diameter of MII oocytes may vary substantially (Fig. 24) but it is not related to fertilization or developmental quality of human ICSI embryos at the cleavage stage of development (Romão *et al.*, 2010). The situation is different with giant oocytes (Balakier *et al.*, 2002; Rosenbusch *et al.*, 2002). This type of oocyte has about twice the volume of a normal oocyte (about 200 μm) and is tetraploid before meiosis due to their origin, i.e. nuclear but no cytoplasmic division in an oogonium or cytoplasmic fusion of two oogonia. These mechanisms explain the binucleate appearance of

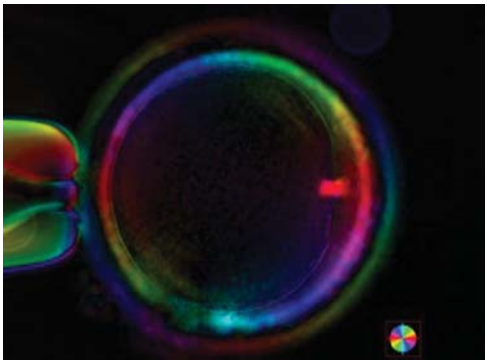

Figure 21 Telophase I oocyte visualized using polarized light microscopy (400× magnification). PB1 is present in the PVS at the 3 o'clock position; however, the MS is still bridging PB1 and the oocyte cytoplasm indicating that this oocyte is not yet a fully mature MII oocyte.

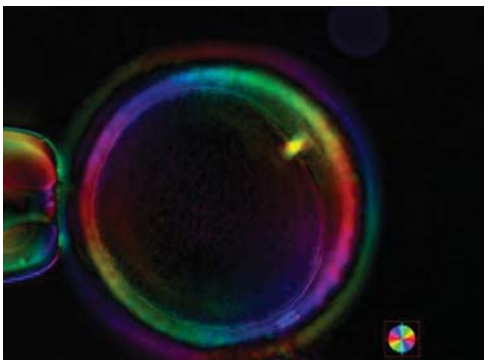

Figure 22 Telophase I oocyte visualized using polarized light microscopy (400× magnification). The MS can be seen between PB1 and the oocyte cytoplasm indicating that this oocyte is still completing the first meiotic division despite the extrusion of PB1 in the PVS.

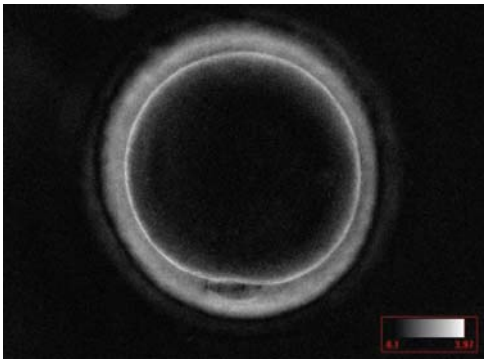

Figure 23 Interphase oocyte (between the first and second meiotic division; Prophase II) visualized using polarized light microscopy (400× magnification). PB1 is present in the PVS at the 6 o'clock position; however, the MS of the second meiotic division is not yet visible in the cytoplasm. This is not yet a fully mature MII oocyte.

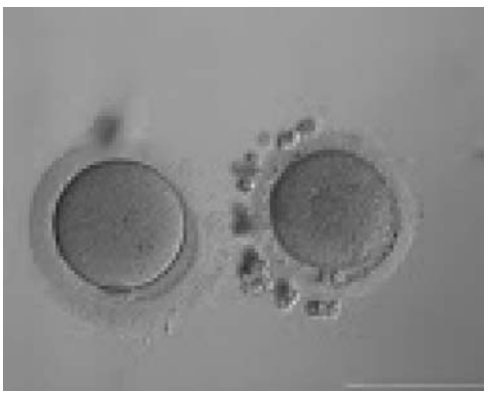

Figure 24 Small MII oocyte (right) next to a normal-sized MII oocyte (left) from the same cohort (200× magnification).

prophase I giant eggs (Figs 25 and 26). These oocytes always contribute to digynic triploidy (Figs 27 and 28) and must never be transferred, although the presence of at least one giant oocyte in a cohort of retrieved eggs (Figs 29 and 30) has no effect on treatment outcome (Machtinger *et al.*, 2011).

It is evident that oocytes with extreme forms of shape anomaly exist (Figs 31 and 32; Paz *et al.*, 2004; Esfandiari *et al.*, 2005). Such ova have been shown to be fertilizable and may lead to the birth of healthy babies. While quantifying the degree of the elongation, some authors (Ebner *et al.*, 2008) realized that the dimensions of the shape anomaly were neither correlated with fertilization nor embryo quality. However, when oocytes with ovoid zonae (Figs 33 and 34) develop, day 2 embryos show a flat array of blastomeres rather than the more traditional tetrahedral arrangement and further development is often delayed (Ebner *et al.*, 2008).

Rarely, two oocytes can be found within the one follicular complex. Each oocyte is usually surrounded by a ZP but the ZP immediately between the two oocytes is commonly shared rather than duplicated (Fig. 35). It is not uncommon for these conjoined oocytes to show different nuclear maturational states. It has been suggested that such oocytes may play a role in producing dizygotic twins; however, even when both of the conjoined oocytes are mature it is rare that both fertilize and no pregnancies have been reported from such oocytes (Rosenbusch and Hancke, 2012).

D. Cytoplasmic features

D.1 Ooplasm

It has been shown in the literature that severe dysmorphisms of the cytoplasmic texture impairs the developmental and implantation potential of the embryo (Balaban and Urman, 2006). Although a

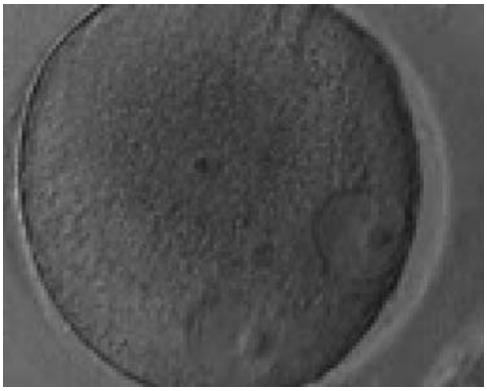

Figure 25 Giant oocyte with two apparent GVs (in an eccentric position). This is a tetraploid oocyte originating from the fusion of two separate oocytes (400× magnification).

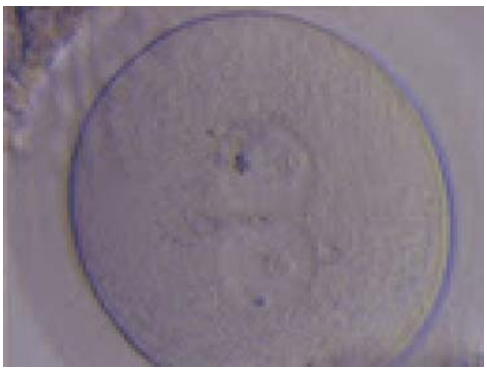

Figure 26 Giant oocyte with two apparent GVs (centrally located and juxtapposed). This tetraploid oocyte originates from the fusion of two separate oocytes and is usually tetraploid (400× magnification).

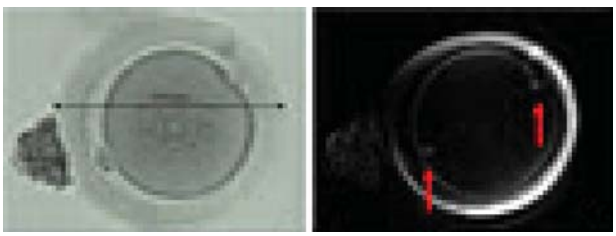

Figure 27 Giant MII oocyte visualized using bright field (left) and polarized light microscopy (right). The oocyte contains two distinct polar bodies and two distinct MSs at opposing poles of the oocyte.

homogeneous, normal cytoplasm is expected in recovered oocytes (Figs 36 and 37), the biological significance of different degrees of heterogeneity in the ooplasm is unknown. Based on current evidence, slightly heterogeneous cytoplasm may only represent normal variability

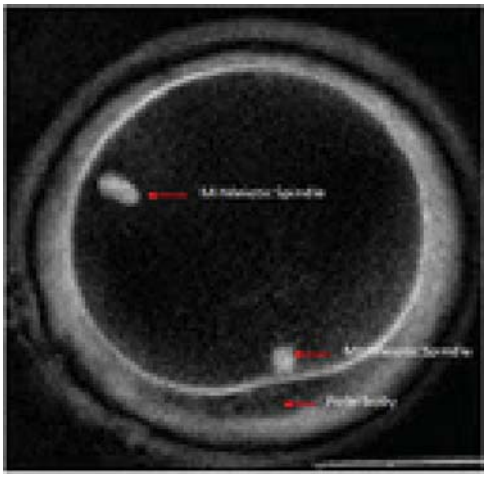

Figure 28 Giant MII oocyte visualized at high power using polarized light microscopy. The two distinct MSs can be observed in the cytoplasm. One MS is from the MI (10 o'clock position) and the other is from MII (6 o'clock position; 400× magnification).

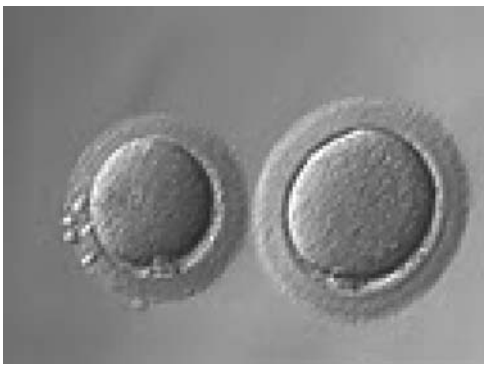

Figure 29 Giant oocyte (right) next to normal-sized oocyte (left; 200× magnification).

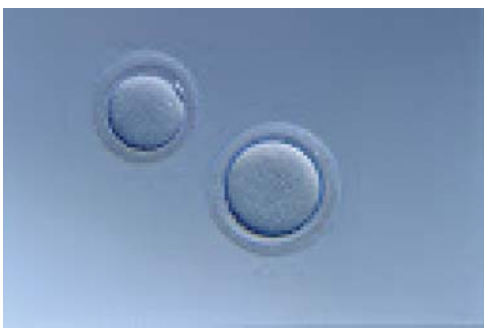

Figure 30 Giant oocyte (right) next to normal-sized oocyte (left; 200× magnification). No PB1 is visible in the giant oocyte.

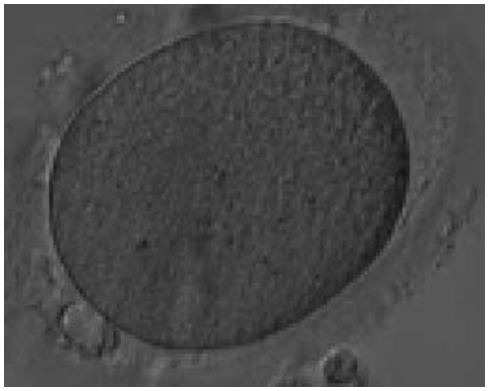

Figure 31 Elongated MII oocyte inside an elongated ZP. Note the PVS appears relatively normal (400× magnification).

Figure 32 Elongated MII oocyte within a grossly distended and irregular ZP (200× magnification).

Figure 33 Ovoid MII oocyte. Note the ZP is also ovoid in appearance and the PVS is enlarged at both poles (200× magnification).

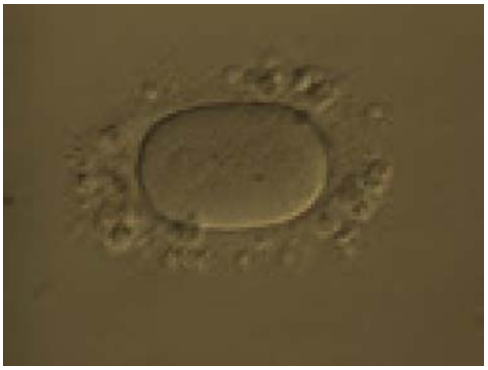

Figure 34 Ovoid MII oocyte. Note the ZP is also ovoid in appearance permitting the PVS to remain relatively normal (200× magnification).

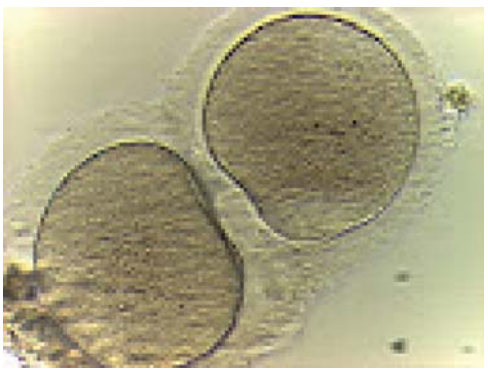

Figure 35 Two oocytes enclosed within a single ZP (400× magnification).

Figure 36 Normal homogenous cytoplasm in an MII oocyte (400× magnification).

Figure 37 Normal homogenous cytoplasm in an MII oocyte (400× magnification). ZP is dense and homogeneous.

Figure 38 MII oocyte with granular cytoplasm (400× magnification). ZP is thicker in the lower-left part of the oocyte in this view.

among retrieved oocytes rather than being an abnormality of developmental significance (Alpha Scientists in Reproductive Medicine and ESHRE Special Interest Group of Embryology, 2011).

Granularities of the cytoplasm (Figs 38–41) are poorly defined in the literature and may depend on the modulation of the optical path used in phase contrast microscopy. These morphological deviations should be carefully distinguished from inclusions such as refractile bodies or lipofuscin bodies (Otsuki *et al.*, 2007; Fig. 42) and organelle clustering which is also described as very condensed centralized granularity detectable by any form of microscopy (Figs 43–45; Alpha Scientists in Reproductive Medicine and ESHRE Special Interest Group of Embryology, 2011).

One of the most important severe cytoplasmic abnormalities of MII oocytes is the appearance of SER clusters (SER discs) within the cytoplasm. SER discs can be identified as translucent vacuole-like structures in the cytoplasm by phase contrast microscopy (Figs 46 and 47). Evidence-based data clearly demonstrates that the embryos derived from oocytes with SER discs are associated with the risk of serious, significantly abnormal outcomes (Balaban and Urman, 2006;

Figure 39 MII oocyte with granular cytoplasm (400× magnification). ZP is also abnormal with marked differences in thickness.

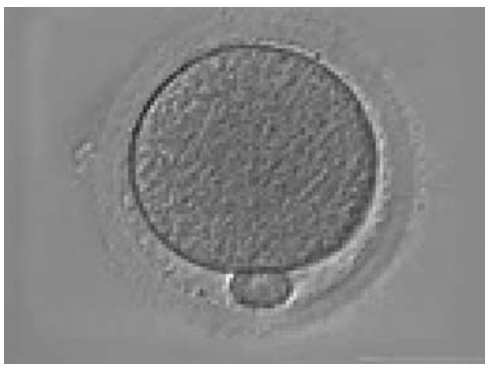

Figure 40 MII oocyte with granular cytoplasm. This figure can be considered as a slight deviation from normal homogeneous cytoplasm (400× magnification).

Figure 41 MII oocyte with a high degree of cytoplasmic granularity/degeneration (400× magnification). PB1 is larger than normal size.

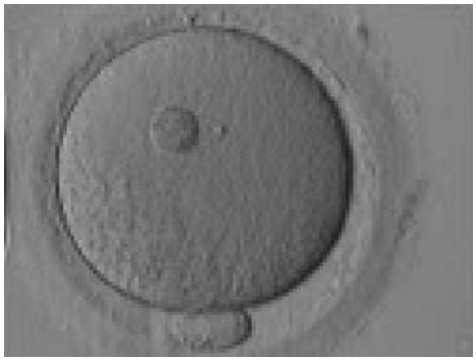

Figure 42 A large refractile body can be seen within the oocyte cytoplasm (400× magnification).

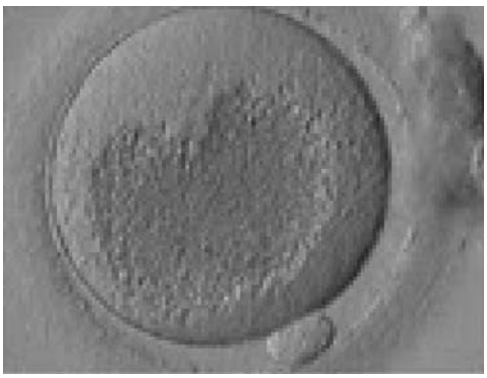

Figure 43 MII oocyte showing a very large centrally located granular area occupying the majority of the cytoplasm. This granularity is typical of organelle clustering.

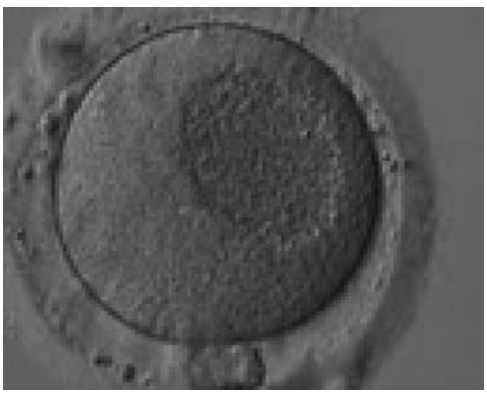

Figure 44 MII oocyte showing a large centrally located granular area in the cytoplasm denoting organelle clustering.

Figure 45 MII oocyte showing organelle clustering forming a large centrally located granular area in the cytoplasm. ZP has an irregular shape.

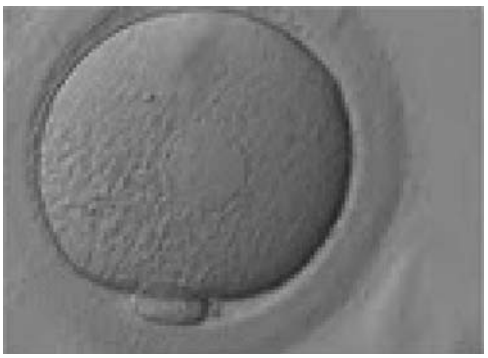

Figure 46 MII oocyte showing plaques of dilated SER discs in the cytoplasm (400× magnification). The SER discs can be clearly distinguished from the fluid-filled vacuoles pictured in Figs 48–51. The cytoplasm looks heterogeneous with granularity (on the left) and areas devoid of organelles toward the 12 o'clock position in this view.

Figure 47 MII oocyte showing plaques of dilated SER discs in the cytoplasm (400× magnification). The PVS is enlarged and PB1 is fragmented.

Figure 48 Vacuolated oocyte. Depicts an oocyte with several small vacuoles distributed throughout the oocyte cytoplasm (200× magnification).

Figure 49 Vacuolated oocyte. This oocyte has a single large vacuole occupying almost half of the oocyte cytoplasm (200× magnification).

Figure 50 Vacuolated oocyte. This oocyte has a single large vacuole in a dark, granular cytoplasm (200× magnification).

Ebner *et al.*, 2006). It is recommended that oocytes with this feature should not be used for injection, and sibling oocytes should be additionally examined for the presence of either a single SER disc or a series of smaller plaques (Alpha Scientists in Reproductive Medicine and ESHRE Special Interest Group of Embryology, 2011).

Vacuoles within the cytoplasm are defined as fluid-filled structures which can be more easily noticeable and differ from SER discs (Figs 48–51). Small vacuoles of 5–10 μm in diameter are unlikely to have a biological consequence, whereas large vacuoles >14 μm are associated with fertilization failure. In oocytes that are fertilized, those vacuoles that persist beyond syngamy can interfere with cleavage planes, resulting in a lower blastocyst rate (Alpha Scientists in Reproductive Medicine and ESHRE Special Interest Group of Embryology, 2011).

D.2 Metaphase plate

It has been shown that the presence of a detectable birefringent MS inside the oocyte cytoplasm of human MII oocytes (Fig. 52) might be an indicator of oocyte quality such as fertilization and

Figure 51 Vacuolated oocyte. Depicts an oocyte with a single small vacuole in the oocyte cytoplasm (400× magnification).

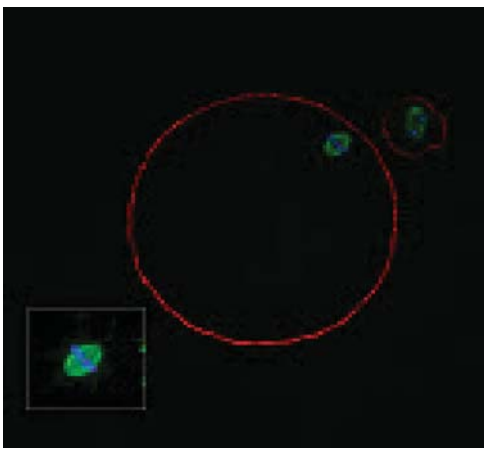

Figure 52 MII oocyte with a normal-shaped MS observed using confocal microscopy.

developmental ability; however, retrospective analysis of results from published articles have been found to be controversial (Borini *et al.*, 2005). A recent meta-analysis showed that although the visibility of the MS of MII oocytes is correlated with fertilization and embryo quality till the blastocyst stage of development, data were insufficient to demonstrate an impairment of the clinical pregnancy and implantation rates (Petersen *et al.*, 2009). The main reason for the controversial findings was that some of the studies did not take into consideration the dynamics of spindle formation that are highly variable during the oocyte maturation stages as well as by confounding technical issues related to oocyte handling. It has been shown that spindle visualization changes during maturation, with a disappearance of the spindle for ~1 h expected during the maturation of MI to PBI extrusion at telophase I and then re-formation at the MII stage. The microtubules of the MS are highly sensitive to chemical (hyaluronidase) and physical changes (temperature and pH variations) that may occur during oocyte handling and a reversible disappearance of the spindle can be expected during these technical preparations (Rienzi *et al.*, 2003; De Santis *et al.*, 2005; Montag *et al.*, 2006).

The spindle structure, when detectable, is not always aligned with the PBI in MII oocytes, and the relationship between the degree of MS deviation from the location of the PBI may also play a role in clinical outcome (Rienzi *et al.*, 2003, 2005; Figs 53–58). Although it has been shown that there is no relationship between the displacement of the PBI with regard to the MS position on fertilization outcomes and embryo quality (Rienzi *et al.*, 2003; Rama Raju *et al.*, 2007), fertilization is impaired when the displacement is >90% (Rienzi *et al.*, 2003; Figs 59 and 60). Slight shifts in the position of the PBI may also be related to physical displacement during the denudation processes, and can be reversible. However, when the displacement is so great because of inappropriate handling, it could cause irreversible damage to the oocyte structure.

Therefore, a precise sequential analysis of MS imaging should be performed after possible chemical and physical changes and immediately prior to ICSI if MS characteristics are to be used as possible markers of oocyte quality and viability.

E. Extracytoplasmatic features

By definition, extracytoplasmic anomalies of the egg include all dysmorphisms related to the ZP, PVS and the polar body of the mature oocyte.

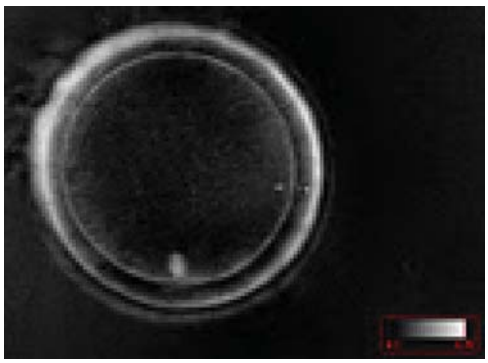

Figure 53 MII oocyte observed using polarized light microscopy with a visible MS just below PB1 (400× magnification).

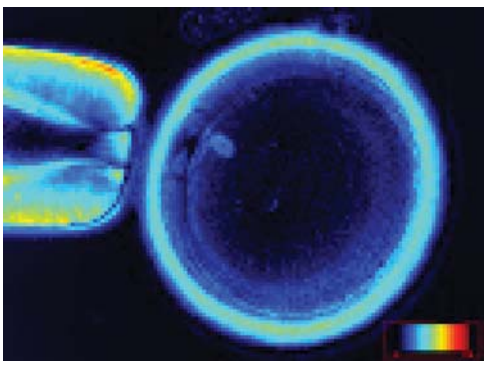

Figure 55 MII oocyte observed using polarized light microscopy with a visible MS just below PB1 that appears fragmented (two fragments). (400× magnification).

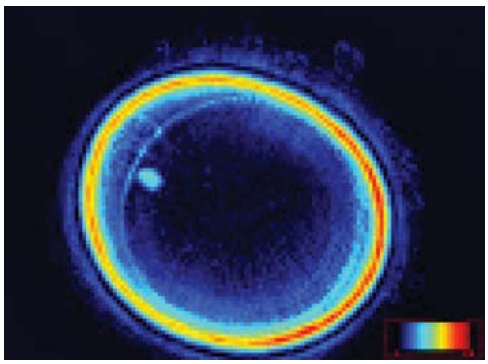

Figure 54 MII oocyte observed using polarized light microscopy with a visible MS near to PB1 (400× magnification).

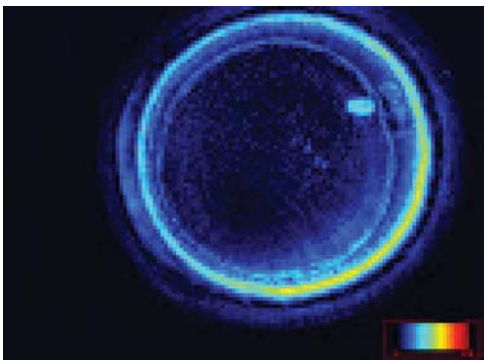

Figure 56 MII oocyte observed using polarized light microscopy. The MS is clearly visible near to PB1 (400× magnification).

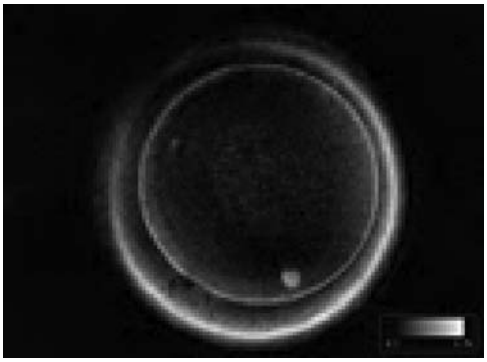

Figure 57 MII oocyte observed using polarized light microscopy with a visible MS slightly dislocated from PB1 at the 7 o'clock position in this view (400× magnification).

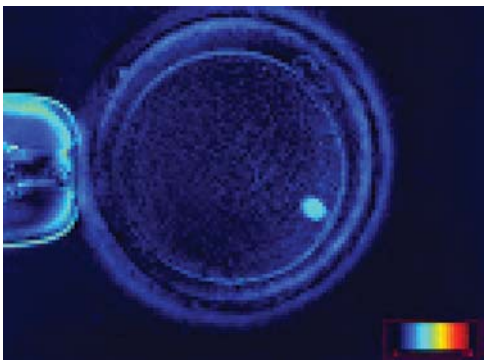

Figure 58 MII oocyte observed using polarized light microscopy with a visible MS dislocated about 80° from PB1 at the 1 o'clock position in this view (400× magnification).

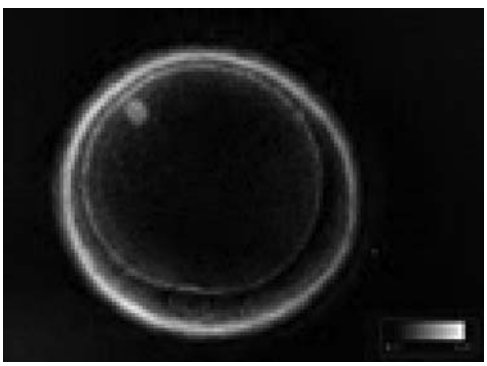

Figure 59 MII oocyte observed using polarized light microscopy with a visible MS highly dislocated (about 135°) from PB1 at the 6 o'clock position in this view (400× magnification).

E.1 Zona pellucida

Any alterations in ZP appearance could be caused by secretion and patterning problems of the glycoprotein matrix (Shen *et al.*, 2005). Since apparent changes in thickness (Figs 61–64) or complete absence of the ZP are extremely rare (Stanger *et al.*, 2001), more subtle changes in the three-dimensional structure are most frequently observed. Since the inner layer of the zona is highly ordered, it can clearly be visualized using polarized light (Figs 65–68; Pelletier *et al.*, 2004). Embryos with a good prognosis in terms of blastocyst formation and pregnancy can be predicted when viewed using polarized light (Montag *et al.*, 2008; Ebner *et al.*, 2010).

The degree to which discoloration of the ZP contributes to the birefringence of the outer shell is not known; however, it has been suggested that successful fertilization, embryo development and pregnancy can be achieved after transfer of embryos derived from brown zonae (Figs 63 and 64; Esfandiari *et al.*, 2006).

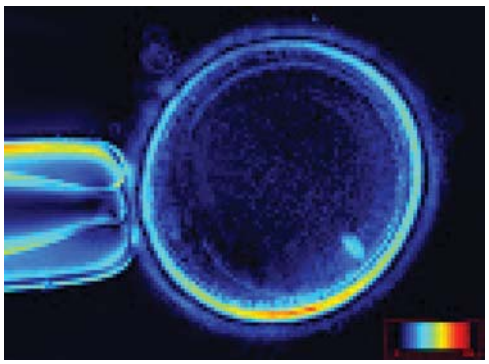

Figure 60 MII oocyte observed using polarized light microscopy with a visible MS highly dislocated (slightly more than 90°) from PB1 at the 8 o'clock position in this view (400× magnification).

Figure 61 MII oocyte with a thick and dense ZP (200× magnification).

Figure 62 MII oocyte with a thick ZP (200× magnification).

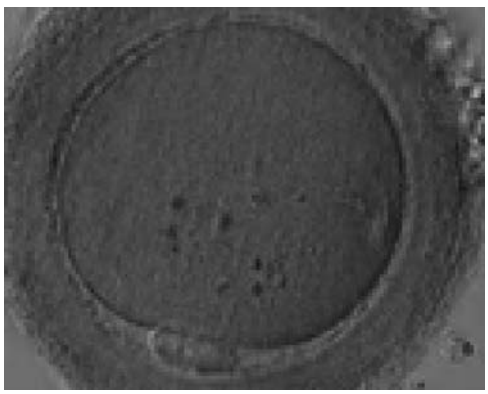

Figure 63 MII oocyte with a thick and dark ZP. Some inclusions are visible in the ooplasm.

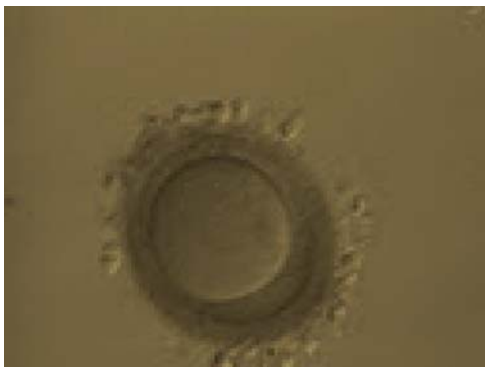

Figure 64 MII oocyte with a thick and dark ZP whose thickness is not homogeneous

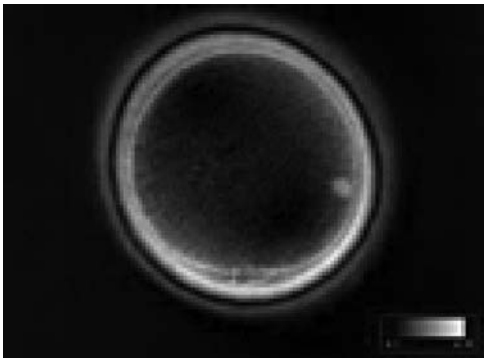

Figure 65 MII oocyte observed using polarized light microscopy with a clear birefringent ZP inner layer. The MS is dislocated from PB1 by almost 90°.

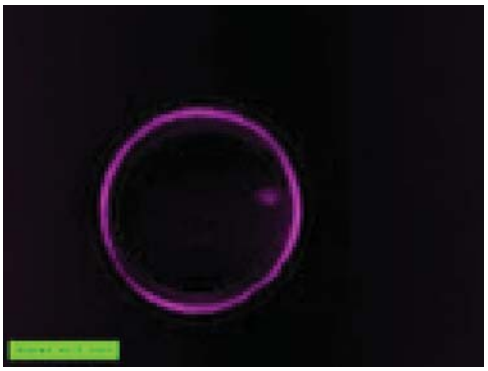

Figure 66 MII oocyte observed using polarized light microscopy with a clear birefringent ZP inner layer. The MS is also clearly visible at the 3 o'clock position in this view.

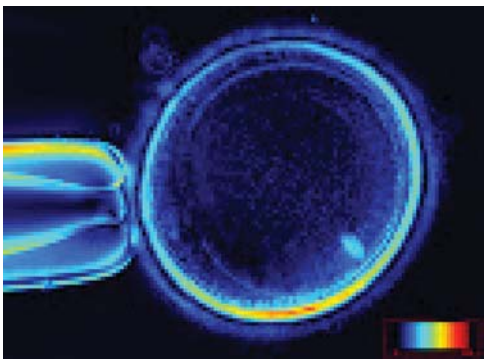

Figure 67 MII oocyte showing different degrees of ZP inner layer birefringence. The figure has a high degree of birefringence.

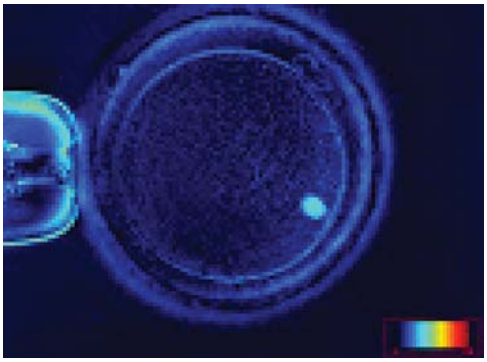

Figure 68 MII oocyte showing different degrees of ZP inner layer birefringence. The figure has a low degree of birefringence.

Figure 69 Oocyte with an abnormally shaped ZP and with what appears to be a duplication of, or tears in, the ZP. The oocyte has an irregular shape and cytoplasmic appearance with a large sized PB1.

Figure 70 Oocyte with an abnormally shaped ZP and with what appears to be a duplication of, or tears in, the ZP. The oocyte is highly dysmorphic with no evident PB1 in the PVS.

Another rare finding is grossly abnormally shaped ZP with what could be either duplication of the inner layer of the ZP or a tear in the layers of the ZP creating an intrazonal space (Figs 69–71).

E.2 Perivitelline space

Several authors have noted that approximately one-third of all ova show a large PVS, a dysmorphism that was found to be negatively correlated with fertilization rate and embryo quality (Xia, 1997; Rienzi *et al.*, 2008). Data from the literature indicate that a large PVS (Figs 72–74) may be ascribed to over-mature eggs (Mikkelsen and Lindenberg, 2001; Miao *et al.*, 2009). In other words, such eggs have shrunk in relation to the ZP presenting a large gap between the oocyte and surrounding zona. A large PVS would also occur if a larger portion of cytoplasm is extruded together with the haploid chromosomal set during PBI formation. This would result in a large PBI and as a consequence a large PVS.

Figure 71 Oocyte with an abnormally shaped ZP and with what appears to be a duplication of, or tears in, the ZP. The oocyte has a regular shape.

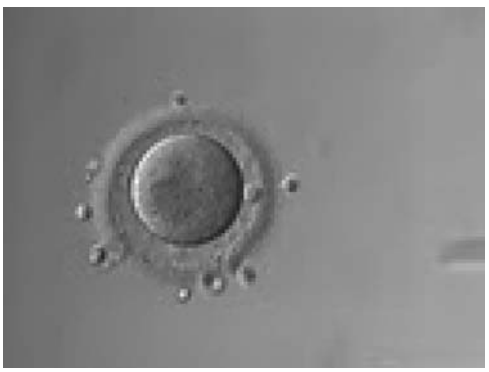

Figure 72 Oocyte with a large PVS. There is a large granular area in the cytoplasm.

Figure 73 Oocyte with a large PVS. Several fragments are present in the PVS.

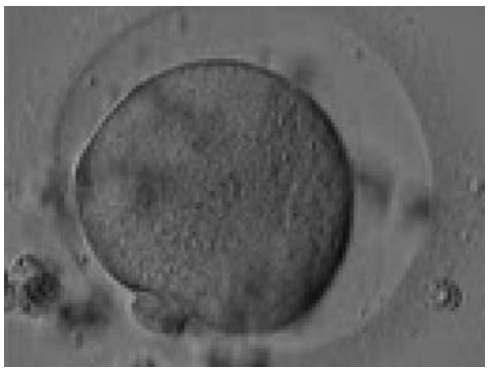

Figure 74 Oocyte with a large PVS and a granular cytoplasm.

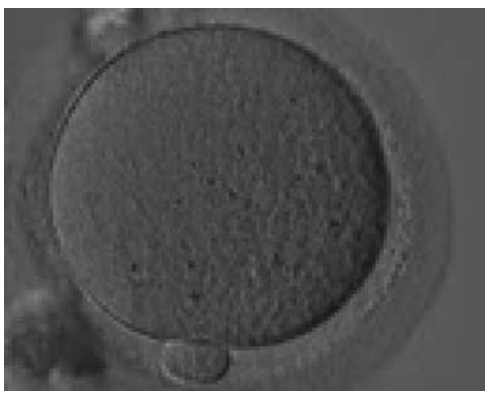

Figure 75 MII oocyte with a normal-sized PBI.

E.3 Polar body

Generally, PBI morphology can be seen as a reflection of postovulatory age of the oocytes since this by-product of meiosis fragments with time. Nevertheless, the impact of PBI morphology on outcome is still a matter of debate. Oocytes showing an intact PBI (Fig. 75) give rise to higher rates of implantation and pregnancy (Ebner *et al.*, 1999) probably due to an increase in blastocyst formation (Ebner *et al.*, 2002). Apparently, the benefit of selecting oocytes according to the morphology of PBI is diluted with increasing time between ovulation induction and ICSI, since studies with different schedules could not find a relationship between morphology of PBI and subsequent ICSI outcome (Ciotti *et al.*, 2004; De Santis *et al.*, 2005; Fancsovits *et al.*, 2006).

However, the fact that a large PBI (Figs 76–78) has a very poor prognosis remains unchallenged (Fancsovits *et al.*, 2006). When large PBI's are extruded, embryos with multinucleated blastomeres are a significantly more frequent consequence than for all other PBI

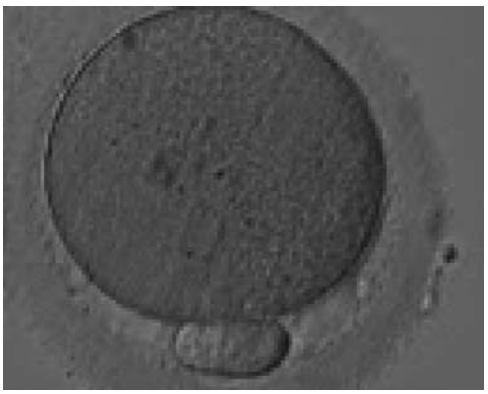

Figure 76 MII oocyte with a large PBI, 3–4 times larger than normal.

Figure 77 MII oocyte with a giant PBI, 5-6 times larger than normal.

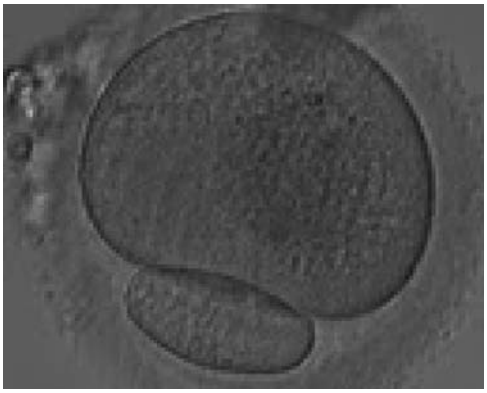

Figure 78 MII oocyte with a giant PBI.

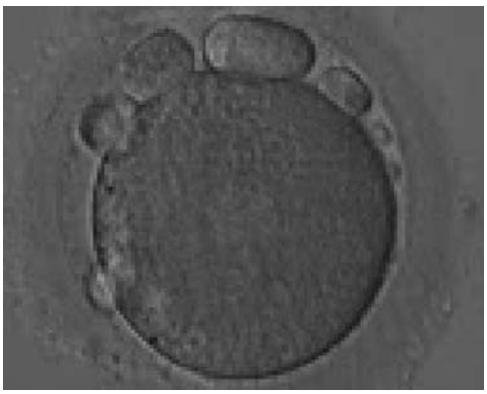

Figure 79 MII oocyte with large fragments and a large PBI in the PVS.

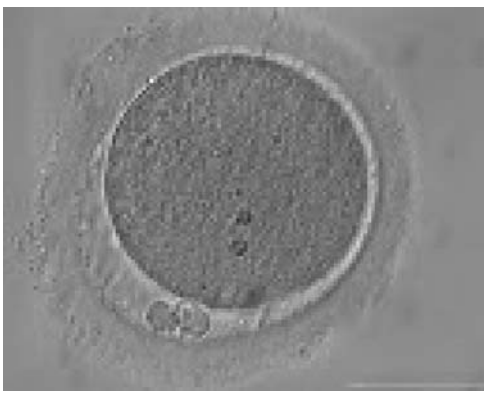

Figure 80 MII oocyte with a fragmented PBI (two pieces).

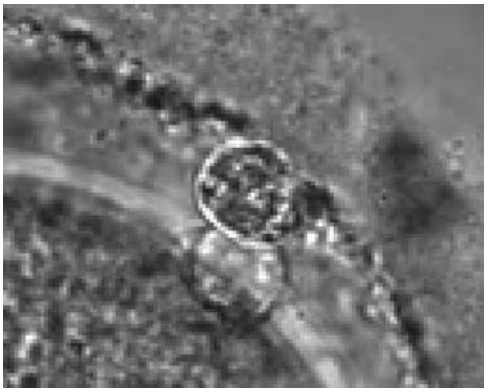

Figure 81 MII oocyte with a fragmented PBI (two pieces) (magnification ×1000).

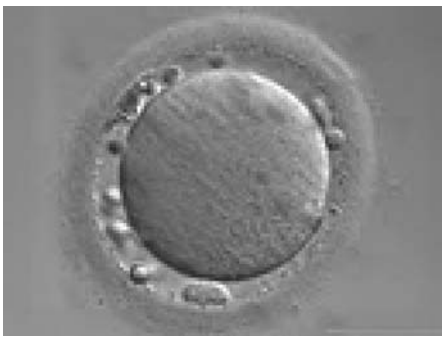

Figure 82 MII oocyte with a fragmented PBI and several cellular fragments within the PVS which are almost indistinguishable from PB1.

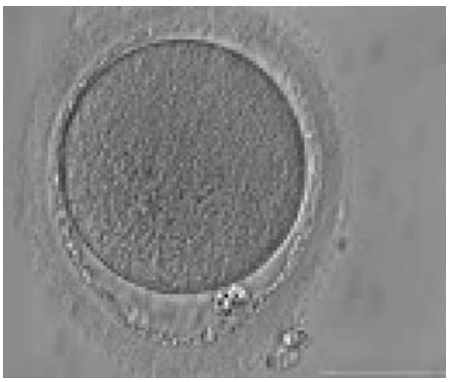

Figure 83 MII oocyte with a lobular/fragmented PBI and significant granulation in the The ZP has a dishomogeneous thickness and an irregular inner layer.

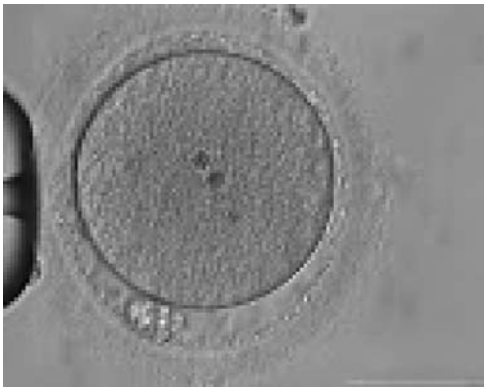

Figure 84 MII oocyte with a lobular/fragmented PBI and significant granulation in the PS. Two inclusion bodies can clearly be seen in the centre of the oocyte.

morphological categories (Fancsovits *et al.*, 2006). It has been postulated that the extrusion of an abnormally large PBI is due to dislocation of the MS (Verlhac *et al.*, 2000).

Sometimes it is difficult to distinguish between heavily fragmented PBI's and debris within the PVS (Figs 79–82). Fertilization and cleavage rate as well as embryo quality have been found to be unaffected by the presence of coarse granules in the PVS (Figs 83 and 84); however, the rates of implantation and pregnancy seem to be influenced (Hassan-Ali *et al.*, 1998; Farhi *et al.*, 2002). Granularity in the PVS has been associated with over-maturity of oocytes (Miao *et al.*, 2009).

References

Albertini DF, Combelles CM, Benecchi E, Carabatsos MJ. Cellular basis for paracrine regulation of ovarian follicle development. *Reproduction* 2001; **121**:647–653.

Alpha Scientists in Reproductive medicine and ESHRE Special Interest Group of Embryology. The Istanbul consensus workshop on embryo assessment: proceedings of an expert meeting. *Hum Reprod* 2011; **26**:1270–1283.

Balaban B, Urman B. Effect of oocyte morphology on embryo development and implantation. *Reprod Biomed Online* 2006;**12**:608–615.

Balaban B, Urman B, Sertac A, Alatas C, Aksoy S, Mercan R. Oocyte morphology does not affect fertilization rate, embryo quality and implantation rate after intracytoplasmic sperm injection. *Hum Reprod* 1998;**13**:3431–3433.

Balakier H, Bouman D, Sojecki A, Librach C, Squire JA. Morphological and cytogenetic analysis of human giant oocytes and giant embryos. *Hum Reprod* 2002;**17**:2394–2401.

Baltz JM, Tartia AP. Cell volume regulation in oocytes and early embryos: connecting physiology to successful culture media. *Hum Reprod Update* 2009;**16**:166–176.

Borini A, Lagalla C, Cattoli M, Sereni E, Sciajno R, Flamigni C, Coticchio G. Predictive factors for embryo implantation potential. *Reprod Biomed Online* 2005;**10**:653–668.

Ciotti PM, Notarangelo L, Morselli-Labate AM, Felletti V, Porcu E, Venturoli S. First polar body morphology before ICSI is not related to embryo quality or pregnancy rate. *Hum Reprod* 2004;**19**:2334–2339.

Cohen Y, Malcov M, Schwartz T, Mey-Raz N, Carmon A, Cohen T, Lessing JB, Amit A, Azem F. Spindle imaging: a new marker for optimal timing of ICSI? *Hum Reprod* 2004;**19**:649–654.

De Santis L, Cino I, Rabellotti R, Calzi F, Persico P, Borini A, Coticchio G. Polar body morphology and spindle imaging as predictors of oocyte quality. *Reprod BioMed Online* 2005;**11**:36–42.

De Sutter P, Dozortsev D, Qian C, Dhont M. Oocyte morphology does not correlate with fertilization rate and embryo quality after intracytoplasmic sperm injection. *Hum Reprod* 1996;**11**:595–597.

Ebner T, Moser M, Yaman C, Feichtinger O, Hartl J, Tews G. Elective transfer of embryos selected on the basis of first polar body morphology is associated with increased rates of implantation and pregnancy. *Fertil Steril* 1999;**72**:599–603.

Ebner T, Moser M, Sommergruber M, Yaman C, Pfleger U, Tews G. First polar body morphology and blastocyst formation rate in ICSI patients. *Hum Reprod* 2002;**17**:2415–2418.

Ebner T, Moser M, Tews G. Is oocyte morphology prognostic of embryo developmental potential after ICSI? *Reprod Biomed Online* 2006; **12**:507–512.

Ebner T, Shebl O, Moser M, Sommergruber M, Tews G. Developmental fate of ovoid oocytes. *Hum Reprod* 2008;**23**:62–66.

Ebner T, Balaban B, Moser M, Shebl O, Urman B, Ata B, Tews G. Automatic user-independent zona pellucida imaging at the oocyte stage allows for the prediction of preimplantation development. *Fertil Steril* 2010;**94**:913–920.

Esfandiari N, Ryan EAJ, Gotlieb L, Casper RF. Successful pregnancy following transfer of embryos from oocytes with abnormal zona pellucida and cytoplasm morphology. *Reprod Biomed Online* 2005;**11**:620–623.

Esfandiari N, Burjaq H, Gotlieb L, Casper RF. Brown oocytes: implications for assisted reproductive technology. *Fertil Steril* 2006;**86**:1522–1525.

Fancsovits P, Tothne Z, Murber A, Takacs FZ, Papp Z, Urbancsek J. Correlation between first polar body morphology and further embryo development. *Acta Biol Hung* 2006;**57**:331–338.

Farhi J, Nahum H, Weissman A, Zahalka N, Glezerman M, Levran D. Coarse granulation in the perivitelline space and IVF-ICSI outcome. *J Assist Reprod Genetics* 2002;**19**:545–549.

Feuerstein P, Cadoret V, Dalbies-Tran R, Guerif F, Bidault R, Royere D. Gene expression in human cumulus cells: one approach to oocyte competence. *Hum Reprod* 2007;**22**:3069–3077.

Gilchrist RB, Lane M, Thompson JG. Oocyte-secreted factors: regulators of cumulus cell function and oocyte quality. *Hum Reprod Update* 2008; **14**:159–177.

Hassan-Ali H, Hisham-Saleh A, El-Gezeiry D, Baghdady I, Ismaeil I, Mandelbaum J. Perivitelline space granularity: a sign of human menopausal gonadotrophin overdose in intracytoplasmic sperm injection. *Hum Reprod* 1998;**13**:3425–3430.

Laufer N, Tarlatzis BC, DeCherney AH, Masters JT, Haseltine FP, MacLusky N, Naftolin F. Asynchrony between human cumulus-corona cell complex and oocyte maturation after human menopausal gonadotropin treatment for *in vitro* fertilization. *Fertil Steril* 1984;**42**:366–372.

Machtinger R, Politch JA, Hornstein MD, Ginsburg ES, Racowsky C. A giant oocyte in a cohort of retrieved oocytes: does it have any effect on the *in vitro* fertilization cycle outcome? *Fertil Steril* 2011;**95**:573–576.

Miao YL, Kikuchi K, Sun QY, Schatten H. Oocyte aging: cellular and molecular changes, developmental potential and reversal possibility. *Hum Reprod Update* 2009;**15**:573–585.

Mikkelsen AL, Lindenberg S. Morphology of in-vitro matured oocytes: impact on fertility potential and embryo quality. *Hum Reprod* 2001; **16**:1714–1718.

Montag M, Schimming T, Van der Ven H. Spindle imaging in human oocytes: the impact of the meiotic cycle. *Reprod Biomed Online* 2006; **12**:442–446.

Montag M, Schimming T, Köster M, Zhou C, Dorn C, Rösing B, van der Ven H, Ven der Ven K. Oocyte zona birefringence intensity is associated with embryonic implantation potential in ICSI cycles. *Reprod Biomed Online* 2008;**16**:239–244.

Montag M, Köster M, Van der Ven K, van der Ven H. Gamete competence assessment by polarizing optics in assisted reproduction. *Hum Reprod Update* 2011;**17**:654–666.

Oldenbourg R. Polarized light microscopy of spindles. *Methods Cell Biol* 1999;**61**:175–208.

Otoi T, Fujii M, Tanaka M, Ooka A, Suzuki T. Oocyte diameter in relation to meiotic competence and sperm penetration. *Theriogenology* 2000; **54**:534–542.

Otsuki J, Nagai Y, Chiba K. Lipofuscin bodies in human oocytes as an indicator of oocyte quality. *J Assist Reprod Genet* 2007;**24**:263–270.

Ouandaogo ZG, Haouzi D, Assou S, Dechaud H, Kadoch IJ, De Vos J, Hamamah S. Human cumulus cells molecular signature in relation to oocyte nuclear maturity stage. *PLoSOne* 2011;**6**:e27179.

Paz G, Amit A, Yavetz H. Case report: pregnancy outcome following ICSI of oocytes with abnormal cytoplasm and zona pellucida. *Hum Reprod* 2004;**19**:586–589.

Pelletier C, Keefe DL, Trimarchi JR. Noninvasive polarized light microscopy quantitatively distinguishes the multilaminar structure of the zona pellucida of living human eggs and embryos. *Fertil Steril* 2004;**81**:850–856.

Petersen CG, Oliveira JBA, Mauri AL, Massaro FC, Baruffi RLR, Pontes A, Franco JG Jr. Relationship between visualization of meiotic spindle in human oocytes and ICSI outcomes: a meta-analysis. *Reprod Biomed Online* 2009;**18**:235–243.

Rama Raju GA, Prakash GJ, Krishna KM, Madan K. Meiotic spindle and zona pellucida characteristics as predictors of embryonic development: a preliminary study using PolScope imaging. *Reprod Biomed Online* 2007; **14**:166–174.

Rienzi L, Ubaldi F. Oocyte retrieval and selection. In: Gardner DK, Weissman A, Howles CM, Shoham Z (eds). *Textbook of Assisted Reproductive Technologies: Laboratory and Clinical Perspectives*, 3rd edn. London, UK: Informa Healthcare, 2009,5–101.

Rienzi L, Ubaldi F, Martinez F, Iacobelli M, Minasi MG, Ferrero S, Tesarik J, Greco E. Relationship between meiotic spindle location with regard to the polar body position and oocyte developmental potential after ICSI. *Hum Reprod* 2003;**18**:1289–1293.

Rienzi L, Ubaldi FM, Iacobelli M, Minasi MG, Romano S, Greco E. Meiotic spindle visualization in living human oocytes. *Reprod Biomed Online* 2005; **10**:192–198.

Rienzi L, Ubaldi FM, Iacobelli M, Minasi MG, Romano S, Ferrero S, Sapienza F, Baroni E, Litwicka K, Greco E. Significance of metaphase II human oocyte morphology on ICSI outcome. *Fertil Steril* 2008; **90**:1692–1700.

Rienzi L, Vajta G, Ubaldi F. Predictive value of oocyte morphology in human IVF: a systematic review of the literature. *Hum Reprod Update* 2011;**17**:34–45.

Romão GS, Araújo MC, de Melo AS, de Albuquerque Salles Navarro PA, Ferriani RA, Dos Reis RM. Oocyte diameter as a predictor of fertilization and embryo quality in assisted reproduction cycles. *Fertil Steril* 2010;**93**:621–625.

Rosenbusch B, Hancke K. Conjoined human oocytes observed during assisted reproduction: description of three cases and review of the literature. *Rom J Morphol Embryol* 2012;**53**:189–192.

Rosenbusch B, Schneider M, Gläser B, Brucker C. Cytogenetic analysis of giant oocytes and zygotes to assess their relevance for the development of digynic triploidy. *Hum Reprod* 2002;**17**:2388–2393.

Shen Y, Stalf T, Mehnert C, Eichenlaub-Ritter U, Tinneberg HR. High magnitude of light retardation by the zona pellucida is associated with conception cycles. *Hum Reprod* 2005;**20**:1596–1606.

Stanger JD, Stevenson K, Lakmaker A, Woolcott R. Pregnancy following fertilization of zona-free, coronal cell intact human ova. *Hum Reprod* 2001;**16**:164–167.

Swain JE, Pool TB. ART failure: oocyte contributions to unsuccessful fertilization. *Hum Reprod Update* 2008;**14**:431–446.

Tartia AP, Rudraraju N, Richards T, Hammer MA, Talbot P, Baltz JM. Cell volume regulation is initiated in mouse oocytes after ovulation. *Development* 2009;**136**:2247–2254.

Ten J, Mendiola J, Vioque J, de Juan J, Bernabeu R. Donor oocyte dysmorphisms and their influence on fertilization and embryo quality. *Reprod Biomed Online* 2007;**14**:40–48.

Van Blerkom J, Henry G. Oocyte dysmorphism and aneuploidy in meiotically mature human oocytes after ovarian stimulation. *Hum Reprod* 1992;**7**:379–390.

Verlhac MH, Lefebvre C, Guillaud P, Rassinier P, Maro B. Assymetric division in mouse oocytes: with or without MOS. *Curr Biol* 2000; **10**:1303–1306.

Xia P. Intracytoplasmic sperm injection: correlation of oocyte grade based on polar body, perivitelline space and cytoplasmic inclusions with fertilization rate and embryo quality. *Hum Reprod* 1997; **12**:1750–1755.